EFFECT OF HEAT TREATMENT ON MAGNESIUM BASED INCLUSIONS IN LOW-CARBON STEEL

Pei Hsien FENG, ZHANG Jian, Weng-Sing HWANG, Yan-Chi PAN

National Cheng Kung University, Department of Materials Science and Engineering, Tainan, Taiwan, wshwang@mail.ncku.edu.tw

Abstract

Acicular ferrite has been used to increase the toughness and strength of low-carbon alloy steel weld metals. Finely dispersed nonmetallic inclusions can serve as nucleation sites for acicular ferrite, and thus reduce the grain size and consequently improve the mechanical properties of steel. In this study, 7 ppm magnesium was added into Al-killed low-carbon steel (SS400) during secondary steelmaking to fine-tune the composition of the steel and obtain fine particles. The hot rolling process of the steel was simulated using a Gleeble 1500 thermal-mechanical simulator to investigate the relationship between heat treatment and the formation of acicular ferrite. Furthermore, the phase constitution and microstructure of SS400 were analyzed using scanning electron microscopy and electron backscatter diffraction. Finally, the optimal heat treatment of SS400 steel for forming acicular ferrite was determined.

Keywords: Acicular ferrite, Magnesium, Inclusion, Heat treatment, Low-carbon steel

1. INTRODUCTION

Acicular ferrite is considered to be one of the most desirable microstructures for improving strength and toughness [1,2]. The transformation of acicular ferrite, which is believed to be intragranularly nucleated bainite, exhibits an incomplete reaction phenomenon [3]. Several studies have supported this conclusion [4,5,6]. Under certain conditions, nonmetallic inclusions can serve as heterogeneous nuclei for fine acicular ferrite [7]. Acicular ferrite plates radiate from the point nucleation sites, creating an unorganized microstructure. Because of the chaotic crystallographic orientation of an acicular ferrite plate, propagating cracks are deflected by it [8]. Many studies have been conducted on acicular ferrite due to its excellent mechanical properties. However, none of these studies used commercial steel.

Table 1 Chemical composition of experiment steel (wt.%)

C	Si	Mn	P	S	N	O	Al	Mg
0.14	0.29	0.99	0.008	0.0017	0.0045	0.002	0.025	0.00077

The present study determines the optimal heat treatment process for commercial low-carbon steel (SS400) with 7.7 ppm magnesium pre-added in the deep deoxidation process. The cooling rate for the transformation of austenite to acicular ferrite and the holding temperature right after cooling were studied to ensure that the reaction had completed.

2. EXPERIMENTAL

2.1 Alloy

The steel used in this study was prepared using a commercial steelmaking process. In the previous work, 7 ppm magnesium was wire-fed into SS400 low-carbon steel in a tank degasser. The molten steel was then continuously casted into a slab with dimensions of 300 mm × 1200 mm × 12000 mm. The slab was machined into plates to remove the rust layer. The chemical composition of the resulting plate is given in **Table 1**. These alloy elements provide suitable hardenability for the formation of acicular ferrite. Magnesium was added as a deoxidizer and for the formation of $MgO•Al_2O_4$ and MgO inclusions.

2.2 Heat Treatments

Twenty cylindrical specimens, 8 mm in diameter and 100 mm in length, were wire-cut from the plates and subjected to heat treatment simulation using a Gleeble 1500 simulator. A specimen with identical diameter and 130 mm in length was also wire-cut for determining the austenite grain size for SS400 steel after retention at 1300 °C for 180 seconds. The simulated heat treatments are shown in **Fig. 1** and listed in **Table 2**.

Table 2 Details of heat treatment simulation for all specimens

Specimen	Cooling Rate(°C /s)	Holding Temp. (°C)
A1	1	650
A2	1	550
A3	1	500
A4	1	450
A5	1	400
B1	5	650
B2	5	550
B3	5	500
B4	5	450
B5	5	400
C1	10	650
C2	10	550
C3	10	500
C4	10	450
C5	10	400
D1	20	650
D2	20	550
D3	20	500
D4	20	450
D5	20	400

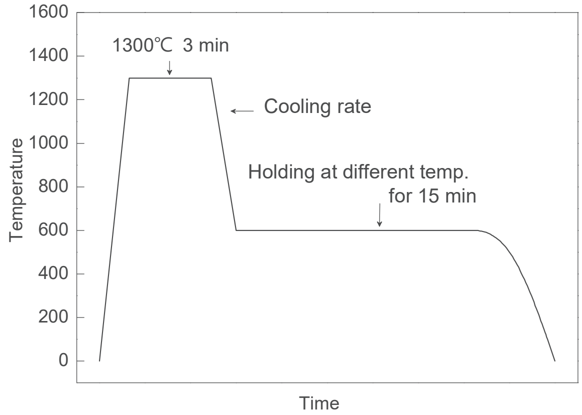

Fig. 1 Heat treatment simulation of SS400 steel on Gleeble 1500

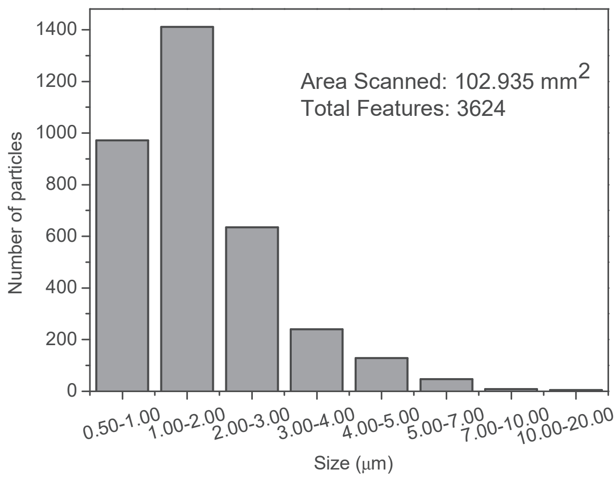

Fig. 2 Size distribution for all inclusions

2.3 Sample Preparation

The sample for inclusion analysis was machined from the slab after continuous casting. It was ground and polished using a 1-μm diamond compound. The composition of the inclusions was examined using FEI/Aspex Explorer. The total area examined was 102.935 mm^2, and the number of inclusions analyzed was 3624.

The microstructure of the heat-affected zone was examined using optical microscopy (OM) and scanning electron microscopy (SEM) with an electron backscatter diffraction (EBSD) analysis system and an energy-dispersive X-ray (EDX) microanalyzer. Samples for OM and SEM were prepared from discs (8 mm in diameter and 3 mm in thickness) machined from the middle of the heat-affected zone. The discs were electropolished in a 75% acetic acid and 25% hypochlorous acid mixture at 25 V and ambient temperature after being ground using sandpaper. Quantitative measurements of the volume fraction of acicular ferrite were carried out using OM under a magnification of 500x. The area examined for each sample was about 1 mm^2.

EBSD analyses were carried out using Zeiss SUPRA SEM for prior-austenite grain size measurement.

3. RESULTS AND DISCUSSION

3.1 Inclusion Analysis

Aspex analysis results show that with 7.7 ppm magnesium addition, the inclusions in SS400 steel are mostly spinel (Al_2O_3•MgO) and MgO. The size distribution for all inclusions is shown in **Fig. 2**.

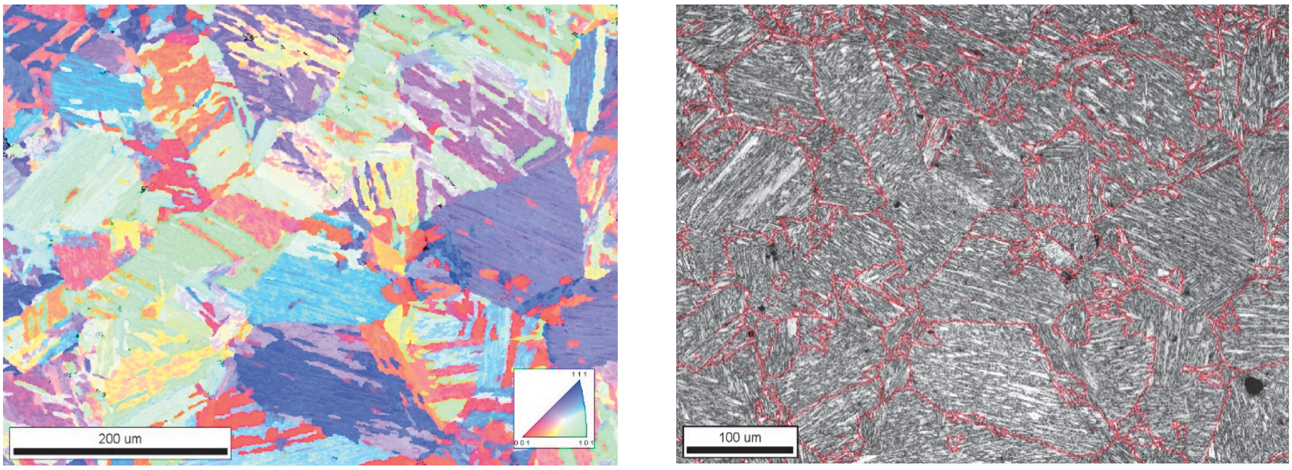

(a) (b)

Fig. 3 (a) IPF image of prior-austenite grain and (b) prior-austenite grain boundary

3.2 Prior Austenite Grain

According to Lee and Pan [9], austenite grain size greatly affects the formation of acicular ferrite. In order to determinate the austenite grain size for SS400 steel after retention at 1300 °C for 180 seconds, the neighbor-to-neighbor [10] method was applied to reconstruct the γ-parent grains for the steel. The EBSD patterns in **Fig. 3-a** and **3-b** show the prior-austenite grain structure of the steel. The sample consists primarily of martensite due to the water quenching right after retention. Using TSL OIM Analysis software, the average grain size was calculated to be 84.04425 μm.

3.2 Microstructure

Twelve optical micrographs were taken for each specimen at magnifications of 200x, 500x, and 1000x after heat treatment simulation on the Gleeble simulator. All steels consisted of acicular ferrite, polygonal ferrite, Widmanstätten ferrite, and bainite. The acicular ferrite preferentially nucleates at the inclusions located within the austenite grain, whereas Widmanstätten ferrite, polygonal ferrite, and bainite usually nucleate at grain boundaries. The optical micrographs show that specimen D4 consists essentially of acicular ferrite. Its primary microstructure is shown in **Fig. 4**.

The heat treatment path for specimen D4 includes the following parameters: peak temperature, T_{peak} = 1300 °C, retention time at 1300 °C, t_{1300} = 180 seconds, cooling rate from 1300 °C to 400 °C, T_{rate} = 20 °C/s, and holding at 400 °C for 15 min. The SEM morphology of acicular ferrite in SS400

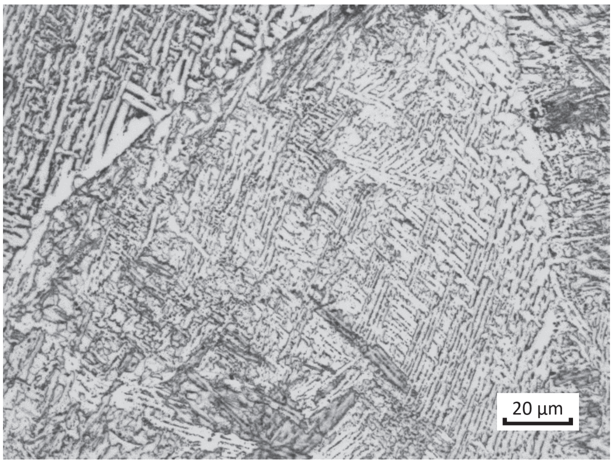

Fig. 4 Optical micrograph showing primary microstructure of D4. The sample consists essentially of acicular ferrite with very little polygonal ferrite and bainite

steel is shown in **Fig. 5**. The acicular ferrite plates nucleated on the MgO-spinel complex inclusion. It has been reported that small platelets of acicular ferrite apparently nucleate sympathetically [11] on other acicular ferrite plates.

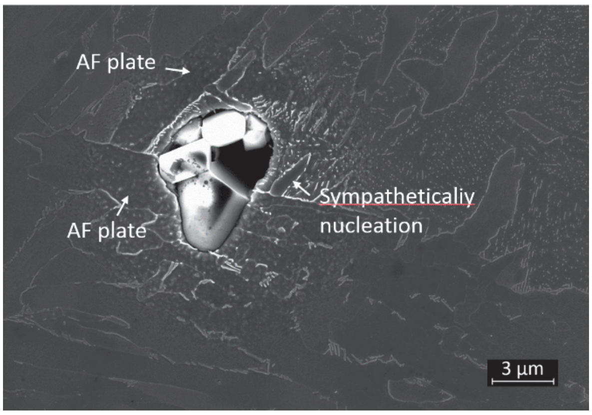

Fig. 5 SEM morphology of acicular ferrite and MgO-spinel complex inclusion.

CONCLUSION

In this study, the optimal heat treatment process for the formation of acicular ferrite for SS400 low-carbon steel with Mg-based inclusions was determined. The heat treatment path is shown in the previous paragraph. The OM images show that the microstructure of sample 4D consists primarily of acicular ferrite plates with some Widmanstätten ferrite and martensite. The SEM images confirm the relationship between Mg-based inclusions and the formation of acicular ferrite plates.

ACKNOWLEDGEMENTS

The authors are grateful to Mr. Chen for provision of Gleeble 1500 simulation machine at China Steel Company, and to the National Science Council of Taiwan, R. O. C., for its financial support of this study under grant NSC 100-2221-E-006-091-MY3. This study also supported by the Ministry of Education, Taiwan, R.O.C. The Aim for the Top University Project to the National Cheng Kung University (NCKU) under grant D103-23014.

REFERENCES

[1] R. A. Farrar and P. L. Harrison, J. Mater. Sci., 1987, 22, pp 3812-3820.

[2] D. J. Abson and R. J. Pargeter, Int. Met. Rev., 1986, 31, pp 141-194.

[3] J. R. Yang and H.K.D.H. Bhadeshia, Adv. in Welding Tech. and Sci., ASM, Ohio, 1987, pp. 187-191.

[4] S.S. Babu and H.K.D.H. Bhadeshia, Mater. Sci. Tech., 1990, 6, pp 1005-1020.

[5] H.K.D.H. Bhadeshia and J. W. Christian, Mater. Metall. Trans. A, 1990, 21A, pp 767-797.

[6] M. Strangwood: Ph.D. Thesis, University Of Cambridge, Cambridge, UK, 1987.

[7] R. A. Ricks, P. R. Howell and G. S. Barritte, J. Mater. Sci., 1982, 17, pp 732-740.

[8] J. R. Yang, C. Y. Huang and C. F. Huang, J. Mater. Sci. Lett., 1993, 12, pp 1290-1293.

[9] J. L. Lee and Y. T. Pan, ISIJ Int., 1995, 35, pp 1027-1033.

[10] C. Cayron, B. Artaud, L. Briottet, Mater. Charact., 2006, 57, pp 386-401.

[11] J. R. Yang and H. K. D. H. Bhadeshia, Mater. Sci. Technol., 1989, 5, pp 93-97.